View Online / Journal Homepage / Table of Contents for this issue
Dynamic Article Links

Organic & Biomolecular Chemistry

Cite this: *Org. Biomol. Chem.*, 2012, **10**, 4782

www.rsc.org/obc

**PAPER**

# Porphyrin-based multi-signal chemosensors for $Pb^{2+}$ and $Cu^{2+}$†

**Yuting Chen**[a,b,c] **and Jianzhuang Jiang***[b,c]

***Received 12th February 2012, Accepted 25th April 2012***
**DOI: 10.1039/c2ob25313e**



Two metal-free tetra(aryl)porphyrin derivatives modified by one and four *N*,*N*-bis(2-pyridylmethyl)amino group(s), namely porphyrin-1-DPA (**1**) and porphyrin-4-DPA (**2**) respectively, have been designed, synthesized, and characterized. Binding with $Pb^{2+}$ induces a significant change in their solution color and in the ratio of two absorption/fluorescence signal peaks, rendering them the first example of porphyrin-based triple-signal optical sensors for $Pb^{2+}$. Their dual-mode $Cu^{2+}$-selective sensing properties *via* either the porphyrin fluorescence ON–OFF mechanism or metal displacement from the **1**–$Pb^{2+}$ complex that results in a triple-signal change clearly reveals their potential application as excellent and versatile sensors.

## Introduction

Chemosensors with high sensitivity and simplicity have attracted increasing interest in recent years. In particular, detecting heavy and transition metal (HTM) ions is important because of their extremely toxic impact on the environment and human health.[1] Various molecular optical sensors using electronic absorption, fluorescent emission, and/or colorimetric signals have been synthesized and applied to detect different species of HTM ions selectively including $Pb^{2+}$, $Cu^{2+}$, $Hg^{2+}$, and $Cd^{2+}$.[2] Most of the reports, however, focused on single-analyte chemosensors with few examples for multi-metal ions.[3] Quinoline-based fluorescent sensors able to detect both $Zn^{2+}$ and $Cd^{2+}$ simultaneously *via* PET and ICT mechanisms, respectively, were developed by Jiang and co-workers.[4] A styryl-Bodipy-based molecular logic sensor with multi-receptors for $Zn^{2+}$, $Ca^{2+}$, and $Hg^{2+}$ was synthesized by Akkaya *et al.*[5] Suzuki reported a "jewel pendant ligand" multi-analyte ($Fe^{3+}$ and $Cu^{2+}$) chemosensor containing three chromogenic units.[6] A small molecular probe for $Zn^{2+}$ and $Hg^{2+}$ based on self-assembly and a metal ion replacement mechanism was prepared by Yang *et al.*[7] Very lately, Jiang and co-workers reported the first porphyrin-Bodipy FRET ratiometric sensor for $Fe^{2+}$ and $Hg^{2+}$.[8] However, a molecular optical sensor for the simultaneous detection of the often co-existing $Pb^{2+}$ and $Cu^{2+}$ ions has not been reported thus far. As a result, developing a versatile molecular optical sensor for synchronously detecting these two metal ions is highly desirable.

The porphyrin chromophore is one of the most promising signaling units for constructing fluorescent sensors due to its advantageous photophysical characteristics, such as pronounced photostability, high extinction coefficient, and tunable fluorescence emission.[9] The central tetrapyrrole moiety of this series of conjugated macrocyclic ligands is also able to act as a good functional receptor for various metal ions due to its strong coordinating ability. As a consequence, extensive investigations have been conducted into porphyrin-based fluorescent sensors.[10] However, exploration of versatile molecular sensors with a porphyrin moiety acting as both the signal chromophore and a multi-analyte receptor has not yet been carried out, to the best of our knowledge.

In the present paper, two new porphyrin derivatives, namely 5-[*p*-*N*,*N*-bis(2-pyridylmethyl)amino-phenyl]-10,15,20-tris(4-*tert*-butylphenyl)porphyrin (Porphyrin-1-DPA) (**1**) and 5,10,15,20-tetra[*p*-*N*,*N*-bis(2-pyridylmethyl) amino-phenyl]porphyrin(Porphyrin-4-DPA) (**2**) were designed and synthesized, Scheme 1. In addition to the optical signaling role, the metal-free tetrapyrrole moiety in **1** and **2** functions as a versatile receptor for both $Pb^{2+}$ and $Cu^{2+}$, along with the peripheral *N*,*N*-bis(2-pyridylmethyl)amine (DPA) unit(s). Interestingly, binding of these two porphyrin compounds with $Pb^{2+}$ directly induced a color change visible to the naked eye and also a remarkable ratio signal change of two absorption–emission peaks. Thus, **1** and **2** are the first examples of porphyrin-based multi-signal optical sensors for $Pb^{2+}$. The dual-mode $Cu^{2+}$-selective approach was implemented in these two compounds *via* a porphyrin fluorescence ON–OFF mechanism and triple-signal metal displacement, revealing their versatile sensing nature.

[a] *Key Laboratory of Coordination Chemistry and Functional Materials in Universities of Shandong, Dezhou University, Dezhou 253023, China*
[b] *Department of Chemistry, University of Science and Technology Beijing, Beijing 100083, China*
[c] *Department of Chemistry, Shandong University, Jinan 250100, China. E-mail: jianzhuang@ustb.edu.cn*

† Electronic supplementary information (ESI) available: $^{1}H$ NMR and $^{13}C$ NMR spectra of compounds **1**, **1Zn**, and **2** in $CDCl_3$, MALDI-TOF mass spectra of these compounds, the electronic absorption and fluorescence emission spectra of **1** and **2**, together with **1Zn** upon addition of different metal ions in $CH_2Cl_2$–MeOH (1 : 1). See DOI: 10.1039/c2ob25313e

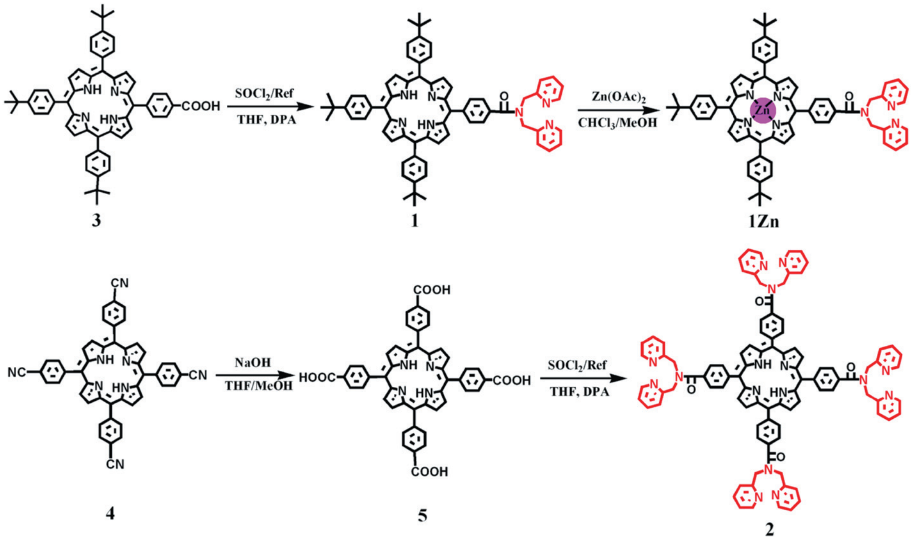

**Scheme 1** Synthesis of DPA-modified porphyrin derivatives **1**, **1Zn**, and **2**.

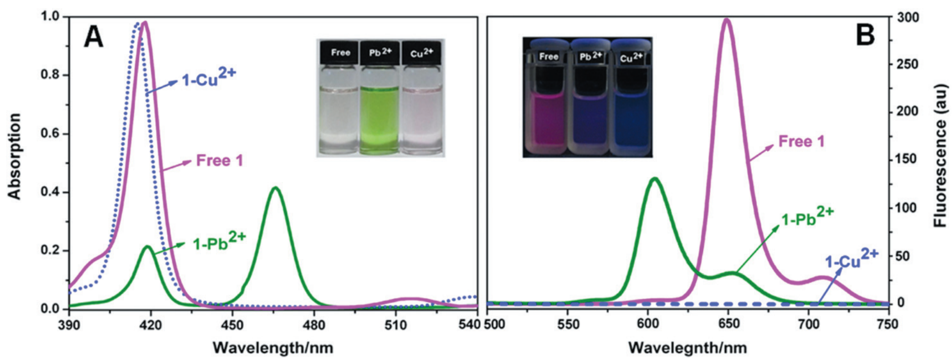


**Fig. 1** The electronic absorption spectra (A) and emission spectra (B) of **1** at the concentration of 2 μM in $CH_2Cl_2$–MeOH (1 : 1) upon addition of $Pb^{2+}$ and $Cu^{2+}$, respectively, with an excitation of 420 nm.



## Results and discussion

As shown in Scheme 1, the synthesis of porphyrin sensors **1** and **2** involved the prior generation of 5-(*p*-carboxylphenyl)-10,15,20-tris (4-*tert*-butylphenyl)porphyrin (**3**) and 5,10,15,20-tetra(*p*-carboxylphenyl)porphyrin (**5**), respectively, in accordance with literature procedures.[11–12] The compounds were refluxed in $SOCl_2$ and treated with DPA in THF. The zinc complex (**1Zn**) was obtained by reaction of the metal-free porphyrin **1** with zinc acetate in a mixed solvent of $CHCl_3$ and MeOH. These three compounds were characterized by MALDI-TOF mass and $^1$H as well as $^{13}$C NMR spectroscopy, Fig. S1–6 (ESI†).

To investigate the selectivity of the metal-free porphyrins for metal ions, the photophysical properties of **1** (2 μM) upon addition of different metal ions, such as $Pb^{2+}$, $Fe^{2+}$, $Co^{2+}$, $Hg^{2+}$, $Mn^{2+}$, $Cu^{2+}$, $Zn^{2+}$, $Ni^{2+}$, $Cd^{2+}$, $Ca^{2+}$, $Ba^{2+}$, $Mg^{2+}$, $Li^+$, $Na^+$, or $K^+$ (10 equiv.), were studied by UV–vis and fluorescence measurements in $CH_2Cl_2$–MeOH (1 : 1). As shown in Fig. 1A, the intensity of the strongest absorption peak of metal-free porphyrin-1-DPA (**1**) at 417 nm significantly decreases upon addition of $Pb^{2+}$. A new peak simultaneously appears around 466 nm, resulting in the $I_{466}/I_{417}$ ratio increasing from 0 to 1.32. Interestingly, the change in the electronic absorption spectrum of **1** upon addition of $Pb^{2+}$ also induces an obvious solution color change from baby pink to light green, Fig. 1A. Meanwhile, a significant change also occurs in the fluorescent emission spectrum of **1** after addition of $Pb^{2+}$. The fluorescent emission intensity of **1** at 650 nm decreases significantly, while a new fluorescent emission peak appears at 604 nm, Fig. 1B. This leads to a change in the ratio of $F_{604}/F_{650}$ from approximately 7576 to 0.26. In addition, the quantitative absorption titration experiments for **1** (2 μM) in $CH_2Cl_2$–MeOH (1 : 1) with increasing amounts of $Pb^{2+}$ (0–10 equiv.) indicate a 1 : 1.5 binding stoichiometry between **1** and $Pb^{2+}$. The approximate association constant ($K_a$) is $2.1 \times 10^4$, which is confirmed by the absorption Job plot and the fluorescent titration experiments, Fig. 2. This suggests a possible binding mode between **1** and $Pb^{2+}$ in **1**–$Pb^{2+}$ system as depicted in Fig. S7A (ESI†). The detection limit for $Pb^{2+}$ ions with **1** was determined to be $3.1 \times 10^{-7}$ M under the present conditions.[13] These results clearly reveal that the metal-free porphyrin-1-DPA **1** can be used for colorimetric and dual

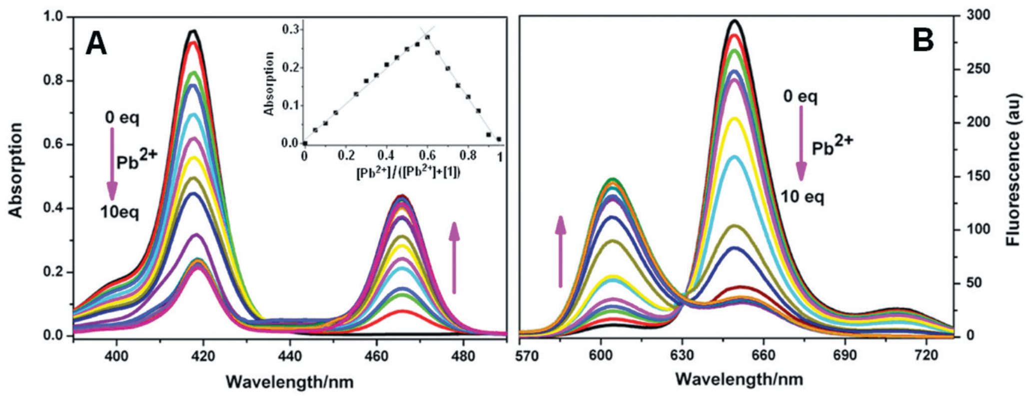


**Fig. 2** The electronic absorption (A) and fluorescent emission spectra (B) of **1** upon addition of increasing amounts (0, 0.2, 0.4, 0.6, 0.8, 0.9 1, 1.2, 1.4, 1.5, 1.6, 1.8, 2, 4, 6, 8, and 10 equiv.) of $Pb^{2+}$, with an excitation of 420 nm. The inset in A shows the 1 : 1.5 binding stoichiometry between **1** and $Pb^{2+}$ in the **1**–$Pb^{2+}$ system at the 466 nm absorption peak.



optical-ratiometric detection of $Pb^{2+}$. It represents the first triple-signal molecular optical sensor for this divalent heavy metal cation.[14]

Addition of $Cu^{2+}$ quenches the fluorescent emission of **1** at 650 nm, but without significantly changing its electronic absorption spectrum, Fig. 1. A quantitative fluorescent titration of **1** with $Cu^{2+}$ shows that the emission intensity at 650 nm gradually decreases to be almost quenched when the amount of $Cu^{2+}$ is increased from 0 to approximately 2.0 equiv., Fig. 3A. Further increases in the amount of $Cu^{2+}$ to 10 equiv. lead to almost no change in the emission spectrum. These results, together with the fluorescence emission Job plot (Fig. 3A), indicate a possible 1 : 2 binding model between **1** and $Cu^{2+}$ with an approximate $K_a$ of 7.4 × $10^5$, Fig. S7B (ESI†). Interestingly, adding $Cu^{2+}$ (10 equiv.) into a solution of **1**–$Pb^{2+}$ ($Cu^{2+}$ : $Pb^{2+}$ = 1 : 1) leads to a rapid color change from light green to baby pink as viewed by the naked eye, Fig. 3B. Electronic absorption spectroscopic measurements confirmed the change from **1**–$Pb^{2+}$ to **1**–$Cu^{2+}$ with the disappearance of the absorption peak at 466 nm and appearance of the absorption peak at 414 nm, Fig. 3B. This suggests the displacement of $Pb^{2+}$ from the **1**–$Pb^{2+}$ complex by $Cu^{2+}$ and the formation of a **1**–$Cu^{2+}$ complex. This hypothesis is further validated by the disappearance of the **1**–$Pb^{2+}$ fluorescence emission peak at 604 nm after addition of $Cu^{2+}$ ions, Fig. S8 (ESI†). The replacement of $Pb^{2+}$with $Cu^{2+}$ can be attributed to the difference in the atomic radius between $Pb^{2+}$ and $Cu^{2+}$. $Pb^{2+}$ has a bigger atomic radius and is located at the periphery of the porphyrin chromophore when binding with the metal-free porphyrin **1**, whereas $Cu^{2+}$ with a smaller atomic radius can be embedded into the central porphyrin core and form a more stable **1**–$Cu^{2+}$ system than **1**–$Pb^{2+}$, resulting in corresponding metal replacement as detailed above. As a consequence, metal-free porphyrin **1** can operate as a dual-mode $Cu^{2+}$-selective sensor *via* the porphyrin fluorescence ON–OFF mechanism as well as the triple-signal (colorimetric, ratio of $A_{414}/A_{466}$, and fluorescence ON–OFF) metal displacement from the **1**–$Pb^{2+}$ complex. Thus, this porphyrin represents a new example of rare dual-mode multi-signal systems for cation recognition,[15] in particular for $Cu^{2+}$ due to its usual paramagnetic fluorescence quenching property.[16]

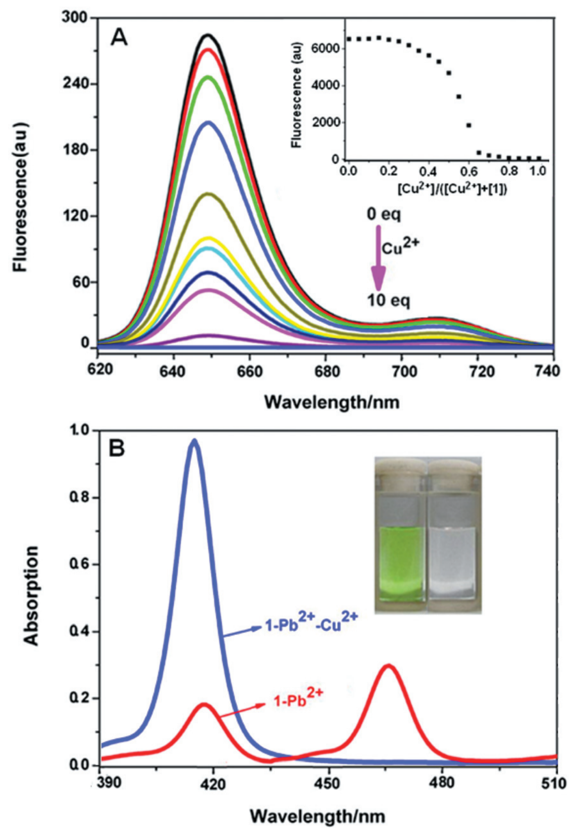


**Fig. 3** The fluorescence emission spectra of **1** (2 μM) in $CH_2Cl_2$–MeOH (1 : 1) upon addition of increasing amounts (0, 0.2, 0.4, 0.6, 0.8, 1, 1.2, 1.4, 1.6, 1.8, 2, 2.2, 2.4, 3, 4, 6, 8, and 10 equiv.) of $Cu^{2+}$ (A), and the electronic absorption spectra and solution color change of **1**–$Pb^{2+}$ upon addition of the same amount of $Cu^{2+}$ ion in $CH_2Cl_2$–MeOH (1 : 1) (B). The inset in A shows 1 : 2 binding stoichiometry between **1** and $Cu^{2+}$ in the **1**–$Cu^{2+}$ system using 650 nm fluorescence emission.

In contrast, upon addition of other metal ions, such as $Fe^{2+}$, $Co^{2+}$, $Hg^{2+}$, $Mn^{2+}$, $Zn^{2+}$, $Ni^{2+}$, $Cd^{2+}$, $Ca^{2+}$, $Ba^{2+}$, $Mg^{2+}$, $Li^+$, $Na^+$, or $K^+$, the electronic absorption and fluorescent emission spectra of the metal-free porphyrin-1-DPA **1** remained almost unchanged, Fig. S9–11 (ESI†). Moreover, addition of these metal ions to the **1**–$Pb^{2+}$ system induces almost no change in either the electron absorption and fluorescent emission spectra, Fig. S8 (ESI†). This is also true for the **1**–$Cu^{2+}$ system, Fig. S12 (ESI†). These results clearly indicate the excellent selectivity of metal-free porphyrin-1-DPA **1** for $Pb^{2+}$ and $Cu^{2+}$ ions over all the tested metal ions.

For the purpose of comparative studies, the electronic absorption and fluorescent emission properties of porphyrin-4-DPA **2** have been investigated in the same manner as for porphyrin **1**. As expected, very similar selectivity and detection properties for $Pb^{2+}$ and $Cu^{2+}$ ions based on the same sensing mechanisms were revealed, Fig. 4A and B and S13–14 (ESI†). However, the quantitative titration experiments for **2** with $Pb^{2+}$ and $Cu^{2+}$ show a binding stoichiometry of 1 : 3 for **2**–$Pb^{2+}$ and of 1 : 5 for **2**–$Cu^{2+}$ due to the increase in the number of peripheral DPA units from one for **1** and four for **2**, Fig. 4C and D and S15 (ESI†). This suggests that the complexes formed with porphyrin **2** have a different binding mode than the complexes formed with porphyrin **1**, as depicted in Fig. 5. Moreover, the observed changes to the optical properties of porphyrin **2** with increasing amounts of $Pb^{2+}$ and $Cu^{2+}$ are smaller in comparison to porphyrin **1**. These results clearly indicate the effect of the number of peripheral DPAs on the detection properties of porphyrin derivatives towards $Pb^{2+}$ and $Cu^{2+}$ cations.

To further understand the sensing properties of these two metal-free porphyrins for $Pb^{2+}$ and $Cu^{2+}$, control experiments with the reference **1Zn** were also carried out under the same experimental conditions. As seen in Fig. S16 (ESI†), addition of

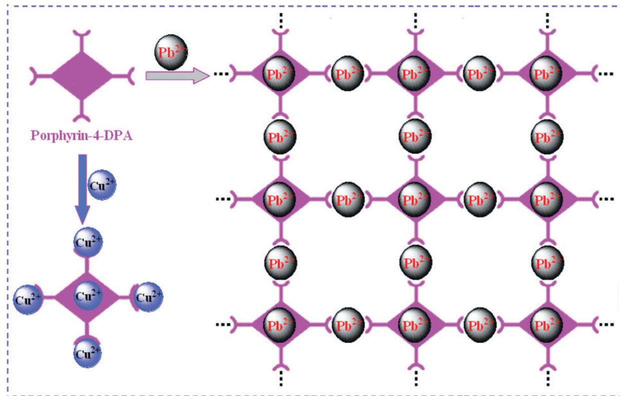


**Fig. 5** The proposed coordinating modes of **2** with $Pb^{2+}$ and $Cu^{2+}$, respectively.

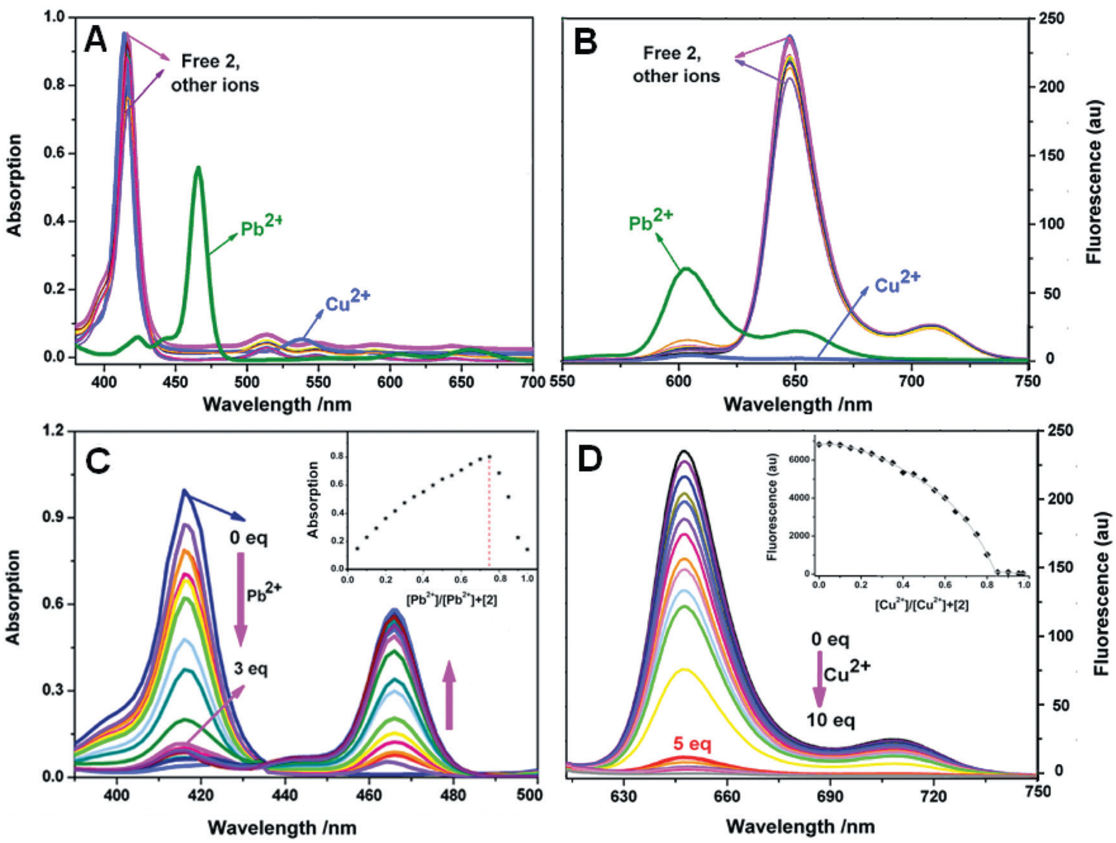


**Fig. 4** The electronic absorption spectra (A) and emission spectra (B) of **2** (2 μM) in $CH_2Cl_2$–MeOH (1 : 1) upon addition of $K^+$, $Li^+$, $Cd^{2+}$, $Ni^{2+}$, $Pb^{2+}$, $Cu^{2+}$, $Mn^{2+}$, $Ba^{2+}$, $Fe^{2+}$, $Co^{2+}$, $Mg^{2+}$, $Ca^{2+}$, $Na^+$, $Hg^{2+}$, or $Zn^{2+}$ (10 equiv.), respectively. The electronic absorption spectra (C) and fluorescent emission spectra (D) of **2** upon addition of increasing amounts of $Pb^{2+}$ and $Cu^{2+}$ (0, 0.2, 0.4, 0.6, 0.8, 0.9 1, 1.2, 1.4, 1.5, 1.6, 1.8, 2, 4, 6, 8 and 10 equiv.), respectively. The insets of C and D show the 1 : 3 and 1 : 5 binding stoichiometry of **2**–$Pb^{2+}$ and **2**–$Cu^{2+}$, respectively, at an excitation of 420 nm.

the various metal ions, including $Pb^{2+}$ and $Cu^{2+}$, into the **1Zn** solution does not induce a remarkable spectroscopic response. This suggests the important role of the coordinating ability of the metal-free porphyrin moiety in determining the excellent sensing properties for $Pb^{2+}$–$Cu^{2+}$. This is further proved by the titration of a *N*-bis(2-pyridylmethyl)amine (DPA) unit with $Pb^{2+}$ and $Cu^{2+}$, which did not show absorption and fluorescence emission in the corresponding optical range. It is worth noting that changes in the optical properties of metal-free 5,10,15,20-tetra-(4-*tert*-butylphenyl)porphyrin upon addition of $Pb^{2+}$ and $Cu^{2+}$were similar to those of **1**, Fig. S17–18 (ESI†). This clearly indicates that the first binding site of the metal-free porphyrin **1** is the central moiety instead of the DPA side group when coordinating with these two metals. Due to the different characteristic outermost electronic structures of $Pb^{2+}$ and $Cu^{2+}$, binding of $Pb^{2+}$ with the central four pyrrole nitrogen atoms in **1** induces a corresponding optical-shift, whereas coordinating with $Cu^{2+}$ results in fluorescent quenching of the porphyrin choromophore. This should also be true for **2**.

## Conclusion

Two metal-free DPA-modified porphyrin derivatives that use the central tetrapyrrole moiety as both the signaling fluorophore and a metal ion receptor have been developed. Significant changes were observed in the solution color, ratio signal of two absorption/fluorescence peaks, and fluorescence intensity of these porphyrin compounds upon their binding with $Pb^{2+}$ and $Cu^{2+}$. When combined with the optical properties associated with $Cu^{2+}$ displacement from **1**/**2**–$Pb^{2+}$ complex, this compound emerges as the first example of a versatile porphyrin-based optical sensor with triple-signal sensing properties for $Pb^{2+}$ and dual-mode fourfold-signaling for $Cu^{2+}$.

## Experimental

### Chemicals

Column chromatography was carried out on silica gel (Merck, Kieselgel 60, 70–230 mesh) with the indicated eluents. THF was freshly distilled from $CaH_2$ under nitrogen. The $CH_2Cl_2$ and methanol used as solvents for the spectral experiments were purified *via* standard methods. Other reagents and solvents were used as received. The compounds of 5-(4-carboxylphenyl)-10,15,20-tris(4-*tert*-butylphenyl)porphyrin (**3**) 5,10,15,20-tetra-(4-cyanophenyl)porphyrin (**4**) and 5,10,15,20-tetra(4-carboxyl-phenyl) porphyrin (**5**) were prepared according to literature procedures.[11–12]

### General instruments

$^{1}H$ and $^{13}C$ NMR spectra ($^{1}H$-400 MHz and $^{13}C$-100 MHz) were recorded on a Bruker DPX 400 MHz spectrometer in $CDCl_3$ with shifts referenced to $SiMe_4$ (0.00 ppm). MALDI-TOF mass spectra were measured on a Bruker BIFLEX III ultra-high resolution Fourier transform ion cyclotron resonance (FT-ICR) mass spectrometer with alpha-cyano-4-hydroxycinnamic acid as the matrix. Elemental analyses were performed on an Elementar Vario El #xX_CYR_HEX_428;. Electronic absorption spectra were recorded on a U-4100 spectrophotometer. Steady-state fluorescence spectroscopic studies were performed on an F 4500 (Hitachi). The slit width was 5 nm for emission. The photon multiplier voltage was 700 V.

### Preparation of 5-[*p*-*N*,*N*-bis(2-pyridylmethyl)amino-phenyl]-10,15,20-tris (4-*tert*-butylphenyl)porphyrin (1)

A mixture of compound **3** (83 mg, 0.1 mmol) and thionyl chloride (10 mL) was refluxed for 5 h under $N_2$ atmosphere and evaporated by atmospheric distillation. The residue obtained was dissolved in THF (8 mL) and then added into a solution of DPA (100 mg, 0.5 mmol) in THF (5 mL), followed by adding two drops of TEA. After stirring for another 4 h at 50 °C, the resulting black–green mixture was evaporated under reduced pressure. The residue was chromatographed on a silica gel column using $CHCl_3$–MeOH (98 : 2) as the eluent, where the second fraction was collected and evaporated. Repeated chromatography followed by recrystallization from $CHCl_3$ and MeOH gave compound **1**, 47 mg in the yield of 46%. $^{1}H$ NMR ($CDCl_3$, 400 MHz) $\delta$ 8.88 (d, 6H, $J$ = 8 Hz), 8.78 (d, 2H $J$ = 4 Hz), 8.69 (d, 1H, $J$ = 4 Hz), 8.62 (br, 1H), 8.23 (d, 2H $J$ = 8 Hz), 8.15 (m, 6H, $J$ = 8 Hz), 7.99 (d, 2H, $J$ = 8 Hz), 7.77 (d, 8H $J$ = 8 Hz), 7.62 (d, 1H, $J$ = 8 Hz), 7.42 (d, 1H, $J$ = 12 Hz), 7.26 (2H obscured by the strong residual $CHCl_3$ signal), 5.08 (d, 4H, $J$ = 4 Hz), 1.61(s, 27H), −2.80 (s, 2H); $^{13}C$ NMR (100 MHz, $CDCl_3$) $\delta$ 172.7, 156.8, 150.5, 150.1, 145.5, 144.1, 139.1, 136.9, 135.1, 125.6, 123.7, 122.7, 122.5, 121.6, 120.6, 120.4, 118.5, 54.9, 50.9, 34.9, 31.7; MS (MALDI-TOF): an isotopic cluster peaking at $m/z$ 1008.49, [Calcd For $M^+$ 1008.53]; Anal. Calcd (%) for $C_{69}H_{65}N_7O$: C, 82.19; H, 6.50; N, 9.72. Found: C, 82.46; H, 6.60; N, 9.34.

### Preparation of 5-[*p*-*N*,*N*-bis(2-pyridylmethyl)amino-phenyl]-10,15,20-tris (4-*tert*-butylphenyl)porphyrinato Zinc complex (1Zn)

$Zn(OAc)_2\cdot 2H_2O$ (33 mg, 0.15 mmol) in MeOH (5 mL) was added into a mixed solution of 5-[*p*-*N*,*N*-bis (2-pyridylmethyl) amino-phenyl]-10,15,20-tris(4-*tert*-butylphenyl) porphyrin (**1**) (100 mg, 0.1 mmol) in $CHCl_3$–MeOH (3 : 1) (30 mL). The reaction mixture was refluxed for 3 h under $N_2$ atmosphere and then diluted with $CH_2Cl_2$ (50 mL). After washing the resulting mixture with an aqueous solution (100 mL) containing EDTA (1 g) and $Na_2CO_3$ (8 g), the organic phase was dried over anhydrous $MgSO_4$, filtered, and evaporated. The residue was chromatographed on a silica gel column using $CHCl_3$–MeOH (98 : 2) as the eluent. Repeated chromatography followed by recrystallization from $CHCl_3$ and MeOH gave compound **1Zn**, 41 mg in the yield of 38%. $^{1}H$ NMR ($CDCl_3$–[$D_5$]pyridine(9 : 1), 400 MHz) $\delta$ 8.77 (d, 5H, $J$ = 8 Hz), 8.65 (d, 2H $J$ = 4 Hz), 8.48 (br, 1H), 8.43 (d, 1H, $J$ = 4 Hz), 8.03 (d, 2H $J$ = 8 Hz), 7.96 (d, 5H, $J$ = 8 Hz), 7.80 (d, 2H, $J$ = 8 Hz), 7.56 (d, 8H $J$ = 8 Hz), 7.44 (d, 1H, $J$ = 4 Hz), 7.26 (1H obscured by the strong residual $CHCl_3$ signal), 7.19 (d, 2H, $J$ = 8 Hz), 7.06 (2H, partly overlapped), 4.92 (d, 4H, $J$ = 8 Hz), 1.41(s, 27H); $^{13}C$ NMR (100 MHz, $CDCl_3$–[$D_5$]pyridine(9 : 1) $\delta$ 172.4, 149.8, 149.7, 149.4, 144.9, 139.9, 136.4, 134.1, 131.5, 131.3, 130.7, 124.8, 123.2, 122.1, 121.9, 121.2, 120.6, 120.3, 118.5, 54.4, 50.3, 34.3, 31.2, 29.2; MS (MALDI-TOF): an isotopic cluster peaking at *m*/*z* 1070.31, [Calcd For $M^+$ 1070.44]; Anal. Calcd (%) for $C_{69}H_{63}N_7OZn$: C, 78.52; H, 6.02; N, 7.85. Found: C, 78.46; H, 6.36; N, 7.34.

### Preparation of 5,10,15,20-tetra[*p*-*N*,*N*-bis(2-pyridylmethyl)-amino-phenyl] porphyrin (2)

The above procedure was used to prepare compound **2** by substituting 5,10,15,20-tetra(4-carboxylphenyl)porphyrin (**5**) (79 mg, 0.1 mmol) for 5-(4-carboxylphenyl)-10,15,20-tris(4-*tert*-butylphenyl)porphyrin (**3**) as the starting material. Compound **2** (42 mg) was obtained with the yield of 27%. $^1$H NMR ($CDCl_3$, 400 MHz) $\delta$ 8.79 (s, 8H), 8.69 (d, 4H, *J* = 4 Hz), 8.63 (d, 4H, *J* = 4 Hz), 8.19 (d, 8H, *J* = 8 Hz), 7.99 (d, 8H *J* = 8 Hz), 7.79 (t, 8H, *J* = 16 Hz), 7.61 (d, 4H, *J* = 8 Hz), 7.42 (d, 4H *J* = 8 Hz), 7.28 (4H, obscured by the strong residual $CHCl_3$ signal), 5.07 (s, 16H), −2.92 (s, 2H); $^{13}$C NMR (100 MHz, $CDCl_3$) $\delta$ 172.5, 157.1, 156.7, 150.1, 149.4, 143.5, 136.9, 135.3, 134.4, 125.7, 122.6, 122.4, 121.7, 119.4, 54.9, 50.9; MS (MALDI-TOF): an isotopic cluster peaking at *m*/*z* 1517.12, [Calcd For $M^+$ 1517.61]; Anal. Calcd for $C_{96}H_{74}N_{16}O_4$: C, 76.07; H, 4.92; N, 14.79. Found: C, 76.35; H, 5.20; N, 14.52.

### Spectroscopic response experiments

Stock methanol solutions (1 mM) of $Hg^{2+}$, $Mn^{2+}$, $Cd^{2+}$, $Ca^{2+}$, $Ba^{2+}$, $Mg^{2+}$, $Li^+$, $Na^+$, and $K^+$ were prepared from their chloride salts, solutions of $Co^{2+}$, $Cu^{2+}$, $Zn^{2+}$, and $Ni^{2+}$ from their acetate salts, the solution of $Pb^{2+}$ from the nitrate salt, and the solution of $Fe^{2+}$ from ferrous ammonium sulfate and used immediately. Solutions of **1**, **2** or **1Zn** (0.2 mM) in $CH_2Cl_2$ were prepared. Test solutions were prepared by placing 0.1 ml of the probe's stock solutions into a test tube, adding an appropriate aliquot of each metal stock solution and then vaporizing the solvents off, followed by diluting the obtained mixture with $CH_2Cl_2$–MeOH (1 : 1, 10 ml) to give the final concentration. After complete mixing for 5 h, UV–vis absorption and fluorescent emission measurements were carried out with a 1 cm standard quartz cell.

## Acknowledgements

Financial support from the Natural Science Foundation of China, Ministry of Education of China, and the Fundamental Research Funds for the Central Universities, the Beijing Municipal Commission of Education, the Fundamental Research Funds for the Central Universities, and the University of Science and Technology Beijing is gratefully acknowledged.

## Notes and references

1 (*a*) M. C. Y. Chang, A. Pralle, E. Y. Chang and C. J. Isacoff, *J. Am. Chem. Soc.*, 2004, **126**, 15392–15393; (*b*) J. Han and K. Burgess, *Chem. Rev.*, 2010, **110**, 2709–2728; (*c*) B. Valeur and I. Leray, *Coord. Chem. Rev.*, 2000, **205**, 3–40; (*d*) X. Zhang, Y. Xiao and X. Qian, *Angew. Chem., Int. Ed.*, 2008, **47**, 8025–8029; (*e*) J. Han, A. Loudet, R. Barhoumi, R. C. Burghardt and K. Burgess, *J. Am. Chem. Soc.*, 2009, **131**, 1642–1643; (*f*) Q. He, E. W. Miller, A. P. Wong and C. J. Chang, *J. Am. Chem. Soc.*, 2006, **128**, 9316–9317; (*g*) H. X. Wang, D. L. Wang, Q. Li, X. Y. Wang and C. A. Schalley, *Org. Biomol. Chem.*, 2010, **8**, 1017–1026.

2 (*a*) S. C. Dodani, Q. He and C. J. Chang, *J. Am. Chem. Soc.*, 2009, **131**, 18020–18021; (*b*) H. Takakusa, K. KiKuchi, Y. Urano, S. Sakamoto, K. Yamaguchi and T. Nagano, *J. Am. Chem. Soc.*, 2002, **124**, 1653–1657; (*c*) D. Srikun, S. E. Miller, D. W. Domaille and C. J. Chang, *J. Am. Chem. Soc.*, 2008, **130**, 4596–4597; (*d*) J. Wang and X. Qian, *Chem. Commun.*, 2006, 109–111; (*e*) Q. He, E. W. Miller, A. P. Wong and C. J. Chang, *J. Am. Chem. Soc.*, 2006, **128**, 9316–9317; (*f*) A. Loudet and K. Burgess, *Chem. Rev.*, 2007, **107**, 4891–4932.

3 (*a*) K. Komatsu, K. Kikuchi, H. Kojima, Y. Urano and T. Nagano, *J. Am. Chem. Soc.*, 2005, **127**, 10197–10204; (*b*) L. Zhang, R. J. Clark and L. Zhu, *Chem.–Eur. J.*, 2008, **14**, 2894–2903; (*c*) E. M. Nolan, J. W. Ryu, J. Jaworski, R. P. Feazell, M. Sheng and S. J. Lippard, *J. Am. Chem. Soc.*, 2006, **128**, 15517–15528; (*d*) K. Hanaoka, K. Kikuchi, H. Kojima, Y. Urano and T. Nagano, *J. Am. Chem. Soc.*, 2004, **126**, 12470–12476; (*e*) Z. Lin, X. Li and H. Kraatz, *Anal. Chem.*, 2011, **83**, 6896–6901.

4 (*a*) L. Xue, C. Liu and H. Jiang, *Org. Lett.*, 2009, **11**, 1655–1658; (*b*) L. Xue, Q. Liu and H. Jiang, *Org. Lett.*, 2009, **11**, 3454–3457.

5 O. A. Bozdemir, R. Guliyev, O. Buyukcakir, S. Selcuk, S. Kolemen, G. Gulseren, T. Nalbantoglu, H. Boyaci and E. U. Akkaya, *J. Am. Chem. Soc.*, 2010, **132**, 8029–8036.

6 H. Komatsu, D. Citterio, Y. Fujiwara, K. Minamihashi, Y. Araki, M. Hagiwara and K. Suzuki, *Org. Lett.*, 2005, **7**, 2857–2859.

7 Z. Wu, Y. Zhang, J. S. Ma and G. Yang, *Inorg. Chem.*, 2006, **45**, 3140–3142.

8 Y. Chen, L. Wan, W. Li, Y. Bian and J. Jiang, *Org. Lett.*, 2011, **13**, 2857–2859.

9 (*a*) J. F. Zhang, Y. Zhou, J. Yoon, Y. Kim, S. J. Kim and J. S. Kim, *Org. Lett.*, 2010, **12**, 3852–3855; (*b*) K. Okamoto and S. Fukuzumi, *J. Am. Chem. Soc.*, 2004, **126**, 13922–13923.

10 (*a*) C. Li, X. Zhang, L. Qiao, Y. Zhao, C. He, S. Huan, L. Lu, L. Jian, G. Shen and R. Yu, *Anal. Chem.*, 2009, **81**, 9993–10001; (*b*) Y. Weng, F. Yue, Y. Zhong and B. Ye, *Inorg. Chem.*, 2007, **46**, 7749–7755.

11 (*a*) X. Y. Zhang, Y. Li, D. D. Qi, J. Z. Jiang, X. Z. Yan and Y. Z. Bian, *J. Phys. Chem. B*, 2010, **114**, 13143–13151; (*b*) Y. Gao, X. Zhang, C. Ma, X. Li and J. Jiang, *J. Am. Chem. Soc.*, 2008, **130**, 17044–17052.

12 (*a*) P. J. F. Gauuan, M. P. Trova, L. Gregor-Boros, S. B. Bocckino, J. D. Crapoc and B. J. Day, *Bioorg. Med. Chem.*, 2002, **10**, 3013–3021; (*b*) T. Giust, D. Gianferrara, I. Bratsos and E. Alessio, *Tetrahedron*, 2007, **63**, 5006–5013.

13 Detection limit (DL) is defined as the concentration corresponding to a signal 3 times the noise level of the background. DL = (0.03 × RSDB)/($x_A/c_0$), where RSDB is both the relative standard deviation of the background expressed as a percent and the sensitivity (the slope of the calibration curve of intensity versus composition), $x_A$ is the net analyte signal (*i.e.*, the signal above background), and $c_0$ is the composition of the element in the sample.

14 (*a*) J. Li and Y. Lu, *J. Am. Chem. Soc.*, 2000, **122**, 10466–1046; (*b*) C. Chen and W. Huang, *J. Am. Chem. Soc.*, 2002, **124**, 6246–6247; (*c*) J. Y. Kwon, Y. J. Jang, Y. J. Lee, K. M. Kim, M. S. Seo, W. Nam and J. Yoon, *J. Am. Chem. Soc.*, 2005, **127**, 10107–10111.

15 M. Royzen, Z. Dai and J. W. Canary, *J. Am. Chem. Soc.*, 2005, **127**, 1612–1613.

16 X. Ni, S. Wang, X. Zeng, Z. Tao and T. Yamato, *Org. Lett.*, 2011, **13**, 552–555.